# Human Motion Reconstruction and Synthesis of Human Skills

Emel Demircan[1], Thor Besier[2], Samir Menon[1], and Oussama Khatib[1]

[1] *Artificial Intelligence Lab., Stanford University, Stanford, CA 94305, U.S.A.,*
[2] *Human Performance Lab., Stanford University, Stanford, CA 94305, U.S.A.,*
*e-mail: emeld, besier, smenon, khatib@stanford.edu*

**Abstract.** Reconstructing human motion dynamics in real-time is a challenging problem since it requires accurate motion sensing, subject specific models, and efficient reconstruction algorithms. A promising approach is to construct accurate human models, and control them to behave the same way the subject does. Here, we demonstrate that the whole-body control approach can efficiently reconstruct a subject's motion dynamics in real world task-space when given a scaled model and marker based motion capture data. We scaled a biomechanically realistic musculoskeletal model to a subject, captured motion with suitably placed markers, and used an operational space controller to directly track the motion of the markers with the model. Our controller tracked the positions, velocities, and accelerations of many markers in parallel by assigning them to tasks with different priority levels based on how free their parent limbs were. We executed lower priority marker tracking tasks in the successive null spaces of the higher priority tasks to resolve their interdependencies. The controller accurately reproduced the subject's full body dynamics while executing a throwing motion in near real time. Its reconstruction closely matched the marker data, and its performance was consistent for the entire motion. Our findings suggest that the direct marker tracking approach is an attractive tool to reconstruct and synthesize the dynamic motion of humans and other complex articulated body systems in a computationally efficient manner.

**Key words:** motion reconstruction, marker space control, musculoskeletal model, human motion synthesis

## 1 Introduction

The reconstruction of human motions is important to researchers who wish to understand the motor strategies skilled humans employ, predict clinical treatment outcomes, or synthesize actor movement in virtual environments. Understanding human motor control involves studying the principles used to optimize movement, and its improvement requires finding changes which make it more optimal. Predicting clinical outcomes of specific biomechanics operations requires developing detailed subject customized models to predict changes in the dynamics as parameters vary. Finally, synthesizing motion involves mapping a subject's motion to a model, overcoming differences in scale, and possibly modifying and mixing motions as they are executed. Motion reconstruction's many objectives make it a challenging task.

Existing reconstruction techniques are application specific, use approximate human models, and usually focus on animating virtual characters to execute tracked motions. The inverse approach estimates the subject's joint angles by imposing motion capture data's spatial and timing constraints to a model and obtains the kinematics or dynamics in joint space [1, 2, 3, 4, 5, 6, 7]. However, estimating joint space from the real world task space translates motion sensing errors into unnatural joint constraints which are further amplified by model imperfections. In addition, inverting motion capture data is computationally expensive. Task space reconstruction [8, 9] overcomes these difficulties by controlling a model to track task space motion capture data directly and obviates the inversion to joint space. Controlling realistic musculoskeletal models in task space to reconstruct motion is challenging due to the many degrees of freedom, their novel singular configurations, and computational efficiency constraints.

In this paper, we applied the task space reconstruction approach to track multiple markers with a detailed subject-customized biomechanical model. To ensure biomechanical detail, we developed a controllable musculoskeletal model based on existing biomechanical models of the upper and lower body [10, 11]. We identified a marker set that constrains the model sufficiently to make its motions match the subject's. We chose a task space marker control hierarchy which tracks markers on the root and leaves of the model's branching structure with the highest priority, and simultaneously tracks intermediate constrained markers in successive null spaces. The higher priority tasks track the motions of the end effectors and pelvis, and the lower priority tasks ensure that the motion of the remaining limbs is consistent with their marker trajectory constraints. Finally, we executed our reconstruction algorithms in our simulation and control framework[12] in near real time.

## 2 Musculoskeletal Motion Reconstruction

For a given desired task, all motion patterns such as body segment location and orientation, balance, posture, collision avoidance [13, 14] need to be specified and controlled in a logical order. They also need to be consistent with physio-mechanical constraints including joint range of motion, singularity avoidance, and muscular effort minimization [9]. To solve these problems, we extend the task-space control framework to marker space, where the marker trajectories are tracked with an accurate musculoskeletal model. The model is scaled to the human subject and is simulated in real-time. The reconstruction process starts with real-time data acquisition using optical marker-based motion capture, and motion data filtering. The musculoskeletal model is then scaled and used to directly track the marker trajectories to obtain the motion dynamics which may be analyzed later.

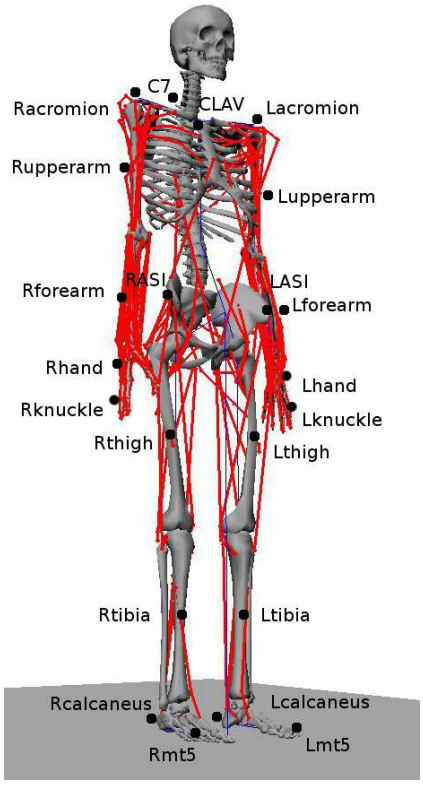


**Fig. 1** The musculoskeletal model scaled and used as the basis for the human motion simulation and reconstruction in our task-level dynamic framework. The 22 markers tracked by our motion reconstruction controller are labeled on the model.

## *2.1 Experimental Procedure and Musculoskeletal Model*

Experiments were conducted using an eight-camera Vicon motion capture system (OMG plc, Oxford UK). A 25-year old healthy left-handed female athlete performed maximum velocity (left-hand) throws of a tennis ball. The motion of the subject was captured at a rate of 120Hz. Following the experiment, the collected position data was processed in Vicon Nexus Software. The raw marker data were filtered using a 15Hz low pass 4th order Butterworth filter.

The musculoskeletal model used in this work combines existing upper [11] and lower [10] body models. The upper body's kinematics contain 15 degrees of freedom which represent the shoulder, elbow, forearm, wrist, and hand. The lower body's kinematics contain 17 degrees of freedom which represent the hip, knee, ankle, subtalar, and metatarsophalangeal joints. The arms-torso, torso-pelvis, and

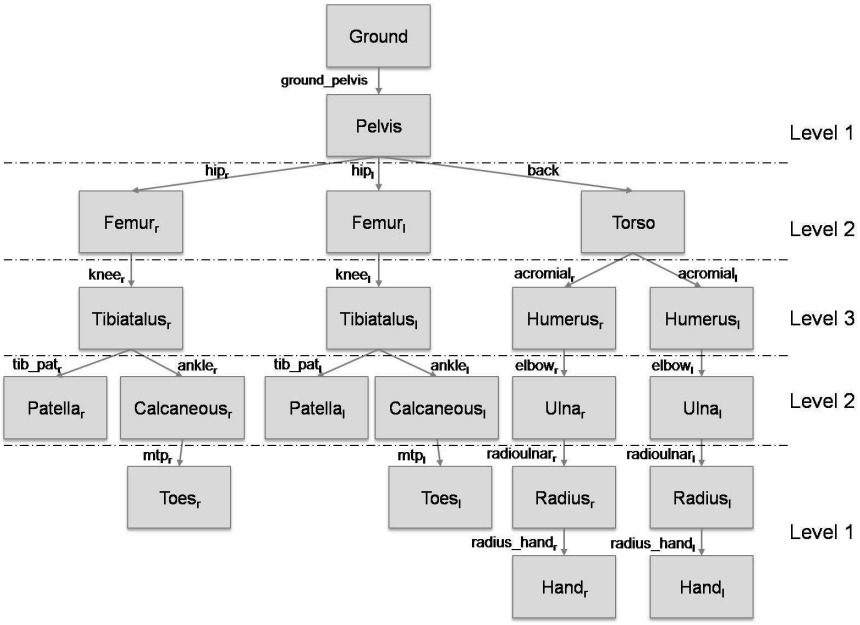


**Fig. 2** The topology of the skeletal model. Each block represents a body segment which is connected to its parent body by the corresponding custom joint. The subscripts *r* and *l* denote the right and left body parts, respectively. The levels correspond to Table 1.

pelvis-leg joints are represented by ball-and-socket joints. The remaining joints are revolute.

The generic human model consists of 20 joints and has 32 degrees of freedom. It was scaled based on body segment mass-center locations [15] to match the anthropometry of the subject. Figure 1 illustrates the scaled musculoskeletal model used in our control and simulation framework and Fig. 2 shows the body segments of the model, each connected to its parent body via the corresponding custom joint. For example, the right ulna is connected to its parent body, right humerus via the right elbow custom joint.

## *2.2 Control Framework*

### 2.2.1 Marker Space Control Formulation

The marker space formulation is constructed by applying an operational space controller [16] to track marker trajectories. The formulation begins with the joint space dynamics of the robot

$$A(q)\ddot{q} + b(q,\dot{q}) + g(q) = \Gamma \tag{1}$$

where $q$ is the vector of $n$ generalized coordinates of the articulated system, $A$ is the $n \times n$ kinetic energy matrix, $b$ is the vector of centrifugal and Coriolis generalized forces, $g$ is the vector of gravity forces, and $\Gamma$ is the vector of generalized control forces.

Task dynamic behavior is obtained by projecting (1) into the space associated with the task, which can be done with the following operation

$$\overline{J}_t^T [A\ddot{q} + b + g = \Gamma] \Longrightarrow \Lambda_t \ddot{x}_t + \mu_t + p_t = \overline{J}_t^T \Gamma \tag{2}$$

Here, $\overline{J}_t^T$ is the dynamically-consistent generalized inverse of $J_t$, the Jacobian of the task, $\Lambda_t$ is the $m \times m$ kinetic energy matrix associated with the task, and $\mu_t$ and $p_t$ are the associated centrifugal/Coriolis and gravity force vectors.

In the operational space framework, the task behavior is divided into a set of independent task points, and the torque component for the task is determined in a manner that compensates for the dynamics in task space. For a task behavior, $x_t$, with decoupled dynamics and unit inertial properties $\ddot{x}_t = F_t^*$, this torque is given by the force transformation

$$\Gamma_{\text{task}} = J_t^T F_t \tag{3}$$

where $J_t$ is the Jacobian of the task and $F_t$ is the operational space force. This operational space control is given by

$$F_t = \Lambda_t F_t^* + \mu_t + p_t \tag{4}$$

where $F_t^*$ is the desired force associated with the task.

In the application to marker space, the task is defined in terms of the markers position coordinates describing the motion capture. The marker space control structure is established as

$$F_{m_i} = \Lambda_{m_i} F_{m_i}^* + \mu_{m_i} + p_{m_i} \tag{5}$$

Here, $F_{m_i}^*$ is the control force associated with $i^{th}$ marker task, and is defined by

$$F_{m_i}^* = \ddot{x}_{m_{i_d}} - k_v(\dot{x}_{m_i} - \dot{x}_{m_{i_d}}) - k_p(x_{m_i} - x_{m_{i_d}}) \tag{6}$$

where $x_{m_{i_d}}$, $\dot{x}_{m_{i_d}}$, and $\ddot{x}_{m_{i_d}}$ denote the desired position, velocity, and acceleration, respectively, associated with the marker tracking task. $k_p$ and $k_v$ are the position and velocity gains. Thus, equation (5) represents the control structure for the trajectory tracking in marker space.

However, the coordinates associated with the positions of markers placed on the articulated body are not all independent. In order to address this dependency, we start by selecting an independent set $m_1$ of markers and a task, $x_{m_1}$, associated with this set. The control of the additional marker task is achieved by projecting the associated control in the null space of the Jacobian matrix associated with $x_{m_1}$.

Dynamic consistency between marker-set tasks is achieved by recursive projections of the associated control torques in the higher priority task null space [17]. For a marker set $m_i$, this is achieved by the dynamically consistent Jacobian $J_{m_i|m_{i-1}|\cdots|m_1}$ defined as

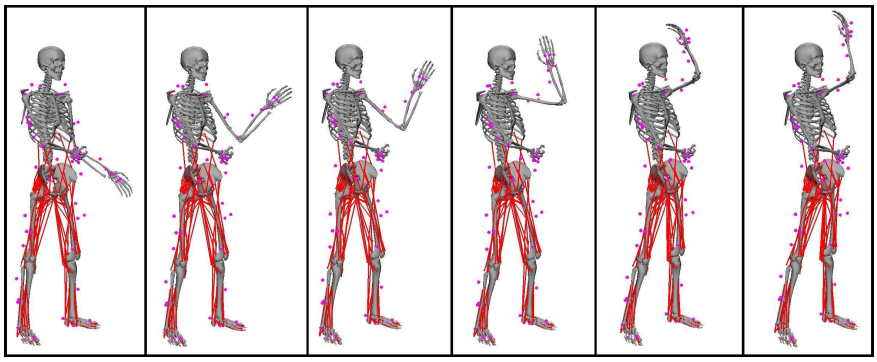

**Fig. 3** A sequence of the reconstructed left hand throwing motion. Note that the dots correspond to the experimental markers attached to the subject.

**Table 1** The hierarchy of the controlled tasks in the marker space. See also Fig. 1 and Fig. 2.

| Level 1 | Level 2 | Level 3 | Level 4 |
|---|---|---|---|
| Pelvis | Torso | Lupperarm | *Posture* |
| Lhand | Lthigh | Rupperarm | *Additional Behaviors* |
| Rhand | Rthigh | Ltibia | |
| Lmt5 | Lforearm | Rtibia | |
| Rmt5 | Rforearm | | |
| LKnuckle | Lcalcaneus | | |
| RKnuckle | Rcalcaneus | | |

$$J_{m_i|m_{i-1}|\cdots|m_1} = J_{m_i} N_{m_{i-1}} \cdots N_{m_1} \tag{7}$$

Where $N_{m_i}$ is the null space associated with the $x_{m_i}$ marker-set task. For $n$ marker-set tasks, the corresponding control torque vector is

$$\Gamma = J_{m_1}^T F_{m_1} + J_{m_2|m_1}^T F_{m_2|m_1} + \cdots + J_{m_n|m_{n-1}|\cdots|m_1}^T F_{m_n|m_{n-1}|\cdots|m_1} \tag{8}$$

### 2.2.2 Human Motion Control Hierarchy

The implementation of the marker space control formulation, described in Sec. 2.2.1, to the human model requires building a hierarchy of independent marker sets. Our approach for assigning markers to these task-sets is based on the observation that two markers can be controlled independently if they are separated by three degrees of freedom that span the space of motion. This principle is applied to the human model following its natural tree-like branching structure. The first level in the task hierarchy is formed by markers placed on the pelvis, its root, and on the hands and feet, its leaves. The following levels are constructed with markers placed on the intermediate links through assignments consistent with the above principle. Addi-

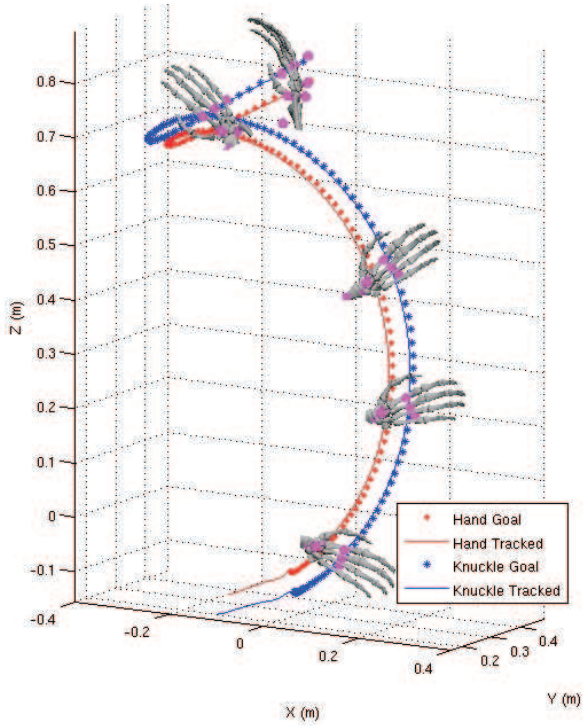


**Fig. 4** Marker trajectories in task space: The left hand and knuckle marker trajectories demonstrate the effectiveness of the task space motion reconstruction algorithm. The markers are tracked while executing a left hand throwing motion. The tracked motion closely follows the recorder marker positions. Placing multiple markers on links (some hidden for clarity) enables the controller to track the position and orientation of the hand well.

tional tasks, such as postures and dissipative forces, are included in the lowest level of the hierarchy.

Table 1 shows the resulting assignment for the human model. Note that the pelvis segment includes both RASI and LASI while the torso segment incorporates C7, CLAV, Lacromion, and Racromion markers that are illustrated in Fig. 1. The independent marker sets are then tracked through the entire movement sequence using this prioritization order. The remaining redundancy is labeled as the posture space of the marker tasks, containing all possible motions that do not affect marker tasks performance. The direct marker control framework allows us to synthesize any additional behavior by projecting its control into the marker task null-space and establishing a new priority.

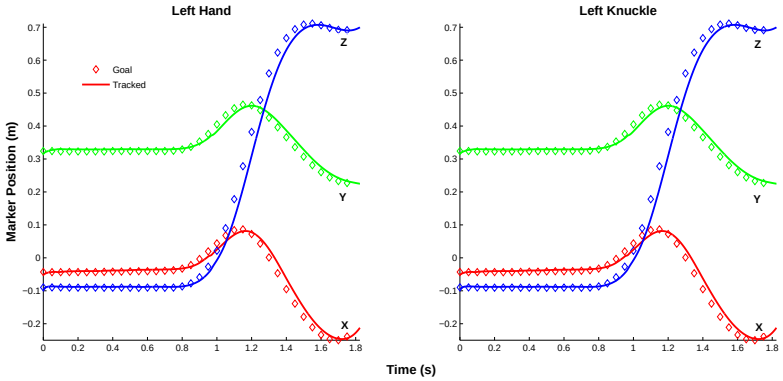


**Fig. 5** Marker trajectories in time: The left hand and knuckle marker trajectories are tracked with little error, even when the motion is fast. While straight line motion is tracked with very low error (1 cm), fast dynamic motions introduce small error overshoots (2–4 cm) since the system is mildly underdamped.

## 3 Results and Real-Time Simulation

The motion reconstruction algorithm presented in Sec. 2.2.1 was tested on a sequence of human throwing motion described in Sec. 2.1 (Fig. 3). The reconstruction was executed by controlling the tasks in three-level marker space (Table 1) formed by independent sets of 22 experimental marker trajectories (see Fig. 1 and Table 1).

Desired and reconstructed trajectories for the throwing(left) hand were recorded during the simulation. Figure 4 illustrates the configurations of the throwing hand together with the desired and reconstructed hand trajectories. Figure 5 shows the reconstructed marker trajectories in time. Trajectory components (x, y and z) of the desired and reconstructed motions were given for both throwing left hand and left knuckle.

The results demonstrate the effectiveness of the reconstruction algorithm by tracking the trajectories with little error (0-4cm). Our principal error source is the scapular elevation and depression of the left shoulder, which are not taken into account in the current human model. The error could be reduced by incorporating the movement of the scapula into the model. Overall, the results show that fast dynamic motions can be effectively reconstructed in near real-time.

## 4 Conclusions

We described our direct marker space control framework for reconstructing human motions by tracking captured marker trajectories with a simulated musculoskeletal model. The reconstruction was performed by successive projections into the null spaces of all tasks that are above it in the hierarchy formed in marker space. A control hierarchy which allows whole-body motion reconstruction was established and tested on a sequence of human throwing motions. Our framework provides an efficient way to map motion patterns to accurate musculoskeletal models without the need for inverse kinematics computations. It also runs in real-time. Our foremost limitation is modeling inaccuracy. For instance, the elevation and depression of the scapula, which enables the shoulder to translate, is not included in the model. The missing scapula movement limits the freedom of the shoulder in fast motions, and its absence dramatically degrades reconstruction near the limits of the arm's workspace.

Our marker space reconstruction methodology provides the full motion dynamics by operating in marker space and automatically resolving the kinematic constraints of the markers. The framework has been used to analyze high performance human motion such as that of athletes and martial art masters [9]. If we control a subset of the limbs, our controller will predict optimal motions for the remaining limbs which can then be used to train subjects. Novel gaits that minimize the knee adduction moment can be predicted by subject-specific musculoskeletal modeling and trained using multi-modal feedback. Similarly, external knee loading that may lead to a non-contact anterior cruciate ligament (ACL) injury during running and cutting maneuvers can be estimated [18, 19], and new altered motion patterns with decreased loads on the knee joint can be modeled in this framework.

**Acknowledgements** The financial supports of the Simbios National Center for Biomedical Computing Grant (http://simbios.stanford.edu/, NIH GM072970) and Honda Company are gratefully acknowledged. The authors would like to thank Rebecca Shultz and Amy Silder for their assistance with the motion capture experiments. Many thanks to Roland Philippsen for his help during the preparation of the paper.

## References

1. Lee J., Shin S. Y.: A hierarchical approach to interactive motion editing for human-like figures. In: Proceedings of the 26th Annual Conference on Computer Graphics and Interactive Techniques, pp.39–48. ACM Press/Addison Wesley Publishing Co. (1999)
2. Choi, K., and Ko, H.: On-line Motion Retargetting. Seventh Pacific Conference on Computer Graphics and Applications, pp.32. IEEE Computer Society (1999)
3. Savenko, A., Clapworthy, G.: Using Motion Analysis Techniques for Motion Retargetting. Sixth International Conference on Information Visualization, **iv**, pp.110. IEEE Computer Society Press (2002)
4. Nakamura, Y., Yamane, K., Suzuki, I., and Fujita, Y.: Dynamic Computation of Musculo-Skeletal Human Model Based on Efficient Algorithm for Closed Kinematic Chains, Proceed-

ings of the 2nd International Symposium on Adaptive Motion of Animals and Machines. Springer, New York (2003)
5. Grochow, K., Martin, S. L., Hertzmann, A., Popovic, Z.: Style-based inverse kinematics. In: ACM Transactions on Graphics (TOG), Proceedings of the 2004 SIGGRAPH Conference, **23**, no.3 , pp.522-531 (2004)
6. Nakamura, Y., Yamane, K., Suzuki, I., and Fujita, Y.: Somatosensory Computation for Man-Machine Interface from Motion Capture Data and Musculoskeletal Human Model. IEEE Transactions on Robotics, **21(1)**, pp. 58–66 (2005)
7. B. Dariush, M. Gienger, B. Jian, C. Goerick, and K. Fujimura: Whole body humanoid control from human motion descriptors. In: IEEE Int. Conf. on Robotics and Automation, pp. 2677–2684 (2008)
8. Demircan, E., Sentis, L., De Sapio, V., and Khatib, O.: Human motion reconstruction by direct control of marker trajectories. In: Jadran, L., Wenger, P. (eds.) Advances in Robot Kinematics (ARK), pp. 263-272. Springer, Verlag New York Inc. (2008)
9. Khatib, O., Demircan, E., DeSapio, V., Sentis, L., Besier, T., Delp, S.: Robotics-based Synthesis of Human Motion. Journal of Physiology - Paris. **103**, pp. 211–219 (2009)
10. Delp, S.L., Loan, J.P., Hoy, M.G., Zajac, F.E., Topp, E.L., Rosen, J.M. : An interactive graphics-based model of the lower extremity to study orthopaedic surgical procedures. IEEE Transactions on Biomedical Engineering **37**, 757–767 (1990)
11. Holzbaur, K.R.S., Murray, W.M., and Delp, S.L: A Model of the Upper Extremity for Simulating Musculoskeletal Surgery and Analyzing Neuromuscular Control. Ann. of Biomed. Eng. **33**, 829–840 (2005)
12. Khatib, O., Brock, O., Chang, K., Conti, F., Ruspini, D., Sentis, L.: Robotics and Interactive Simulation. Communications of the ACM, **45**, no. 3, pp.46–51 (2002)
13. Khatib, O., Sentis, L., Park, J., Warren, J.: Whole-Body Dynamic Behavior and Control of Human-Like Robots. International Journal of Humanoid Robotics. **1**, no. 1, pp.29–43 (2004)
14. Sentis, L., Khatib, O.: Synthesis of Whole-Body Behaviors Through Hierarchical Control of Behavioral Primitives. International Journal of Humanoid Robotics, **2(4)**, pp.505–518 (2005)
15. Dempster, W. T. Space requirements of the seated operator. WADC Technical Report, pp.55-159. Wright-Patterson Air Force Base, OH (1955)
16. Khatib, O.: A unified approach for motion and force control of robot manipulators: The operational space formulation. International Journal of Robotics Research, **3(1)**, pp.43-53 (1987)
17. Khatib, O.: Inertial properties in robotic manipulation: An object level framework. International Journal of Robotics Research, **14(1)**, pp.19–36. (1995)
18. Besier, T. F., Lloyd, D. G., Ackland, T. R., and Cochrane, J. L.: External loading of the knee joint during running and cutting manoeuvres. Medicine in Science and Sports and Exercise. **33:7**, pp.1168–1175 (2001)
19. Besier, T. F., Lloyd, D. G., Ackland, T. R., and Cochrane, J. L.: Anticipatory effects on knee joint loading during running and cutting manoeuvres. Medicine in Science and Sports and Exercise. **33:7**, pp1176–1181 (2001)